Neutron unbound states in ^{28}Ne and ^{25}F

J. K. Smith, T. Baumann, B. A. Brown, G. Christian, J. E. Finck, C. R. Hoffman, Z. Kohley, S. Mosby, J. F. Novak, S. J. Quinn, J. Snyder, A. Spyrou, M. J. Strongman, and M. Thoennessen

(MoNA Collaboration)

Neutron Unbound States in ^{28}Ne and ^{25}F

J.K. Smith,[1,2,*] T. Baumann,[1] B.A. Brown,[1,2] G. Christian,[1,2] J.E. Finck,[3] C.R. Hoffman,[4,5] Z. Kohley,[1] S. Mosby,[1,2] J.F. Novak,[1,2] S.J. Quinn,[1,2] J. Snyder,[1,2] A. Spyrou,[1,2] M.J. Strongman,[1,2] and M. Thoennessen[1,2]

(MoNA Collaboration)[†]

[1]*National Superconducting Cyclotron Laboratory, Michigan State University, East Lansing, MI 48824, USA*
[2]*Department of Physics and Astronomy, Michigan State University, East Lansing, MI 48824, USA*
[3]*Department of Physics, Central Michigan University, Mt. Pleasant, MI 48859, USA*
[4]*Physics Division, Argonne National Laboratory, Argonne, Illinois 60439, USA*
[5]*Department of Physics, Florida State University, Tallahassee, Florida 32306, USA*

Unbound states in ^{28}Ne and ^{25}F were populated in the reaction of a 102 MeV/nucleon ^{29}Na beam on a beryllium target. The measured decay energy of 32(22) keV in the ^{27}Ne + n system corresponds to an unbound excited state in ^{28}Ne at 3.86(11) MeV. This is the first measured unbound state of ^{28}Ne. The decay energy of the ^{24}F + n system was measured as 300(170) keV. This places the second measured unbound state of ^{25}F at 4.66(17) MeV.

PACS numbers: 20.21.10.-k, 20.27.30.+t, 20.29.30.Hs

With the increased availability of rare isotope beams, the neutron-rich landscape has become more accessible, especially for the lighter isotopes. A particular research focus has been to determine the bound or unbound nature of nuclei along the dripline and measure their masses. The neutron dripline has only been mapped up to $Z = 8$ and the study of unbound states of these neutron-rich isotopes have revealed important nuclear structure information [1]. The unbound structure of the most neutron-rich isotopes with $Z > 8$ has not been studied until recently, when Frank *et al.* and Christian *et al.* measured unbound excited states in the bound neutron-rich fluorine isotopes $^{25-27}$F and also reported the first mass measurement of the unbound fluorine nucleus, ^{28}F [2–4]. ^{27}Ne recently became the heaviest bound neon isotope with a measured unbound state [5]. This paper reports on the measurement of two new neutron-unbound states of bound nuclei in that region: the first measured unbound state in ^{28}Ne and the second measured unbound state in ^{25}F.

The experiment was performed at the National Superconducting Cyclotron Laboratory at Michigan State University. A secondary beam consisting of 6% ^{26}F and 94% ^{29}Na was produced by the fragmentation of a 140 MeV/u ^{48}Ca primary beam on a 987 mg/cm^2 Be production target. Analysis of the ^{26}F beam has been previously reported in Refs. [6–9]. The ^{29}Na beam used for the present analysis was identified on an event-by-event basis by time of flight and then reacted on a 470 mg/cm^2 Be reaction target in the experimental area. Charged fragments from the reaction were deflected by the Sweeper magnet [10] into a suite of charged particle detectors while the neutrons were detected by the Modular Neutron Array (MoNA) [11, 12]. The detector setup has been previously described in Ref. [13]. Charged frag-
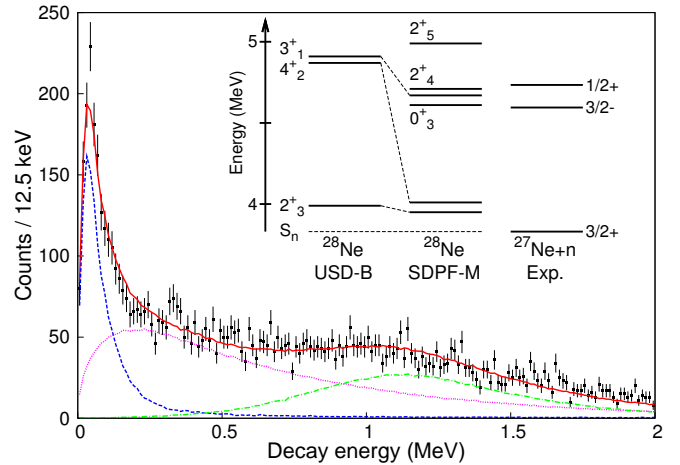
FIG. 1. (Color online) ^{28}Ne decay energy spectrum and best fit to data. The simulated lineshape includes a 32 keV resonance (dashed blue line), a high-lying s-wave lineshape with -2 fm scattering length (dotted purple line), and a high-lying resonance at 1.15 MeV with a fixed width of 200 keV (dot-dashed green line). Inset is a level scheme showing the measured bound states for ^{27}Ne and theoretical calculated unbound states in ^{28}Ne.

ments from the reaction were identified based on their time of flight, energy loss, emittance, and total kinetic energy as reported in Ref. [13]. The measured decay energy spectra for ^{28}Ne and ^{25}F were reconstructed from the ^{27}Ne + n and ^{24}F + n systems, respectively, using an inverse map for the charged particles and the invariant mass method as described in Ref. [14].

Each decay energy spectrum was fitted with a lineshape from a Monte Carlo simulation that included secondary beam characteristics; target thickness; a Glauber reaction model; and detector location, geometry, and resolution. Secondary beam parameters were selected to reproduce the position and angle of the incoming beam while reaction parameters were selected to match the

measured position and angular distributions of the final fragments. Energy-dependent Breit-Wigner [15] and s-wave lineshapes [16] were used to fit the resonant decays, while any non-resonant background was fitted with a Maxwellian distribution. Best fits to the data were determined by χ^2-analysis, with the resonance energy (or scattering lengths) and yields of each component as the only free parameters.

The decay energy spectrum and best fit for ^{28}Ne $\rightarrow$ ^{27}Ne $+ n$ are shown in Figure 1. One low-lying resonance is immediately identifiable. This peak can be best fit with an $l = 2$ energy-dependent Breit-Wigner lineshape at 32(22) keV. ^{28}Ne is populated by a simple one-proton removal, thus significant non-resonant background is not expected. The presence of a higher-lying broad distribution must then be due to several unresolved resonances. Two lineshapes were included to fit the higher-lying broad distribution, an $l = 2$ resonance near 1 MeV and an s-wave lineshape to fit the shoulder near 300 keV. The width of the $l = 2$ resonance near 1 MeV was fixed at 200 keV, its approximate single-particle width as calculated in a Woods-Saxon potential. The location of the 32 keV resonance was insensitive to variations of the fits of these higher resonances. The best fit was achieved with the 32(22) keV resonance, an s-wave lineshape with a scattering length of -2 fm, and a higher-lying resonance of 1.15 MeV. With a neutron separation energy of 3.83(11) MeV [17] and the assumption of decay to the ground state, the 32(22) keV resonance is interpreted as an unbound state at an excitation energy of 3.86(11) MeV, with the majority of the uncertainty coming from the mass uncertainties of ^{28,27}Ne.

Shell model calculations in the sd model space were performed for ^{28}Ne using the NuShellX code [18] and the USD-B [19] interaction. Cross-shell neutron excitations have been necessary to describe bound states in this region, due to the proximity of ^{28}Ne to the island of inversion [20–24]. Thus, Monte Carlo shell model calculations using the SDPF-M interaction [25] have also been performed [26]. The SDPF-M interaction uses a modified sd–pf space and accounts for the mixing of $0\hbar\omega$ and $2\hbar\omega$ configurations up to 5 MeV. This interaction was specifically chosen because wavefunctions consisting of 49% intruder configurations are needed to describe the ground state of the beam, ^{29}Na [27]. The results of both calculations, as well as the experimentally known states are shown in Figure 2. The one-proton removal from ^{29}Na principally populates positive parity states ($C^2S > 0.01$), so the negative parity states calculated with the SDPF-M interaction are not shown.

Calculated spectroscopic overlaps for the one-proton knockout from ^{29}Na to ^{28}Ne are shown in Table I. In the USD-B interaction, only two states in the region of interest are expected to be heavily populated with $C^2S > 0.1$, the 3_1^+ state and the 2_2^+ state. The 3_1^+ state is too high in energy to be attributed to the observed state at 3.86(11) MeV. The 2_2^+ state is calculated as bound, but uncertainties in the measured neutron separation energy (180

TABLE I. Shell model calculations for states in the ^{28}Ne $\rightarrow$ ^{27}Ne $+ n$ system. Columns include spectroscopic overlaps with the ground state of ^{29}Na, spectroscopic overlaps for neutron decay to ^{27}Ne, and single particle and total widths for those decays. All overlaps with ^{27}Ne are overlaps with the $3/2^+$ ground state, with the footnoted exception. The values in the upper half are calculated with the USD-B interaction, while those in the bottom half are calculated with the SDPF-M interaction. Single particle widths for the $l = 2$ neutron decay was calculated for an energy of 32 keV, again with the footnoted exception.

$J^\pi(^{28}\text{Ne})$	$C^2S_{29\rightarrow28}$	$C^2S_{28\rightarrow27}$	$\Gamma_{\rm sp}$ (keV)	Γ (keV)
2_2^+	0.1572	$s_{1/2}$: 0.0002	1200	0.2
		$d_{5/2}$: 0.0008	0.04	0.0003
		$d_{3/2}$: 0.8143	0.04	0.03
2_3^+	0.0285	$s_{1/2}$: 0.0292	1200	35
		$d_{5/2}$: 0.0107	0.04	0.0004
		$d_{3/2}$: 0.0363	0.04	0.001
4_2^+	0.0535	$d_{5/2}$: 0.0006	0.04	2×10^{-5}
3_1^+	0.2102	$d_{5/2}$: 0.0010	0.04	4×10^{-5}
		$d_{3/2}$: 0.0917	0.04	0.004
		$d_{5/2}$: 0.0004[a]	119[b]	0.05
2_2^+	0.343	$s_{1/2}$: 0.004	1200	5
		$d_{5/2}$: 0.012	0.04	0.0005
		$d_{3/2}$: 0.337	0.04	0.01
2_3^+	0.043	$d_{3/2}$: 0.022	0.04	0.0009
		$d_{5/2}$: 0.003	0.04	0.0001
4_2^+	0.237	$d_{5/2}$: 0.002	0.04	9×10^{-5}
2_4^+	0.047	$s_{1/2}$: 0.003	1200	4
		$d_{5/2}$: 0.005	0.04	0.0002
		$d_{3/2}$: 0.809	0.04	0.03
		$d_{5/2}$: 0.055[a]	119[b]	7

[a] Calculated for the decay to the $1/2^+$ excited state at 885 keV.
[b] $\Gamma_{\rm sp}$ calculated for an energy of 917 keV.

keV) and the calculation of shell model energies ($\sim$300 keV) allow for the possibility that the state is slightly unbound. In the SDPF-M model, that same 2_2^+ state is expected to be populated, but its calculated energy is lowered and it becomes more difficult to argue for its unbound nature. The 4_2^+ state, also lower in energy in the SDPF-M calculations, is also expected to be populated. This state has been identified as bound with the use of gamma-ray spectroscopy [24]. The 2_3^+ and 2_4^+ states are expected to be less populated than the 4_2^+ state by an order of magnitude.

Calculations for the decay of ^{28}Ne are also shown in Table I. To estimate the expected relative contributions of the $l = 0$ and $l = 2$ decays, we calculated the neutron-decay widths for both $l = 0$ and $l = 2$ neutron decays with an energy of 32 keV. Our calculation of the s-wave neutron-decay width is based on $\Gamma = C^2S\,\Gamma_{\rm sp}$, where C^2S is the shell-model spectroscopic factor and $\Gamma_{\rm sp}$ is the single particle neutron-decay width. The s-wave sin-
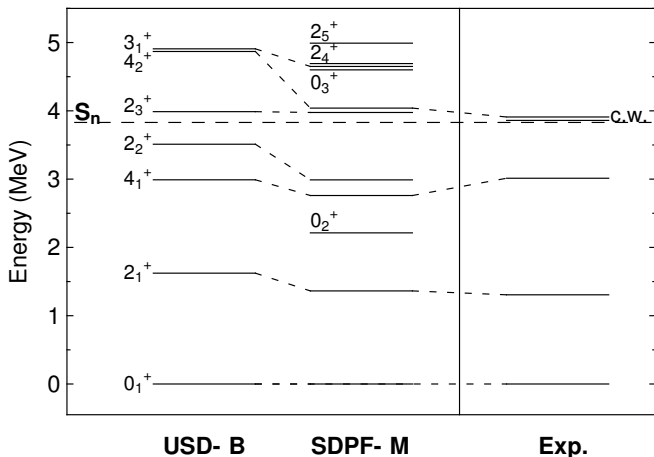
FIG. 2. ^{28}Ne experimental and theoretical calculated levels. Only the positive parity states from the SDPF-M calculation are shown. The horizontal dashed line indicates the one-neutron separation energy from Ref. [17]. The lowest two experimental levels are from Ref. [20]. The highest state, assigned to the 4_2^+ state, is from Ref. [24]. The level marked "c.w.", which is the level presented in the current work, is just above the neutron separation energy.

FIG. 3. (Color online) ^{25}F decay energy spectrum and best fits to data. Top panel simulation includes a 300 keV Breit-Wigner resonance (dashed blue line) and a non-resonant background (dotted purple line). Bottom panel shows a fit that includes the measured resonance from Ref. [2] (filled grey curve) populated at 15% the strength of the population of the resonance.

gle particle neutron-decay width is given by Eq. 3F-51 in Ref. [28]. For ^{28}Ne with $R = 3$ fm we obtain $\Gamma_{sp} = 1.2$ MeV. For the d-wave decay we obtain a single-particle width of 0.04 keV using a Woods-Saxon potential. Spectroscopic overlaps with the $3/2^+$ ground state of ^{27}Ne were calculated for every state in the table. A majority of the resulting decay widths are negligible when compared with experimental resolution, which is approximately 75 keV FWHM at 32 keV decay energy. As a consequence, our sensitivity to the orbital angular momentum of the decay is negligible as well.

In the SDPF-M interaction calculation, the 4^+ state shows a strong overlap ($C^2S = 0.176$ for decay of an $f_{7/2}$ neutron) with a predicted $7/2^-$ state in ^{27}Ne at 25 keV. The parity change would require the emission of an $l = 1, 3$ neutron. Similar to the single-particle widths for an $l = 2$ neutron decay, the widths for an $l = 1, 3$ decay at 32 keV would also render the setup insensitive to angular momentum. This $7/2^-$ state has, however, recently been identified as unbound [5], so we remove it from consideration.

The experiment did not include γ-ray detection, so we cannot rule out that the low energy decay was not to a bound excited state in ^{27}Ne. Two bound states have also been experimentally measured at 765 keV ($3/2^-$) and 885 keV ($1/2^+$) [5, 21], as shown in the inset of Figure 1. Both the 3_1^+ state in the USD-B calculation and the 2_4^+ state in the SDPF-M calculations could decay to these excited states. Non-zero spectroscopic factors and single-particle decay widths for these possible decays are shown in Table I. Based on this analysis, we cannot conclusively assign a
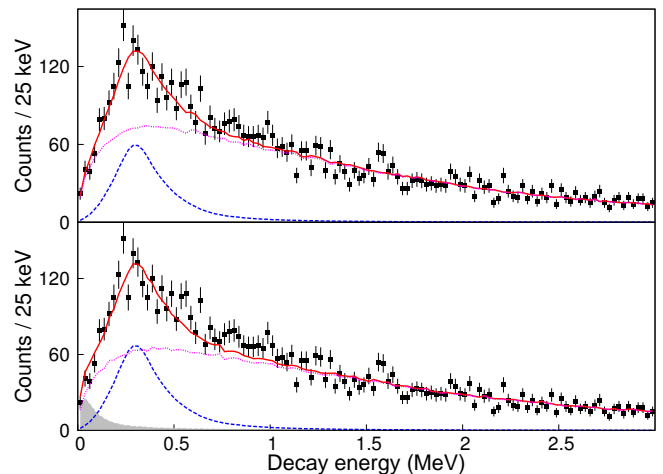
spin to the measured unbound state, but we expect the state to be either 2^+, 3^+, or 4^+.

The multi-step population of ^{25}F is more complicated. Population possibilities include a $2p,2p1n$, or $2p2n$ knockout and subsequent neutron decays to the detected daughter fragment, ^{24}F. In this case, the decay energy spectrum could entirely be due to a Maxwellian non-resonant background from evaporated neutrons from the continuum. The measured spectrum, however, is not fit well by only a non-resonant background; a resonance feature is required for a reasonable fit of the data. The best fit includes an $l = 1$ resonance at 300(170) keV as shown in the top panel of Figure 3. With a neutron separation energy of 4.36(12) MeV [29], this unbound state corresponds to an excited state at 4.66(17) MeV in ^{25}F, once again assuming decay to the ground state.

Shell model calculations were performed for ^{25}F using Oxbash [32] and the WBP [33] interaction in the sp–sd–pf space with the truncations used in Ref. [2]. These calculated levels and the measured experimental levels are shown in Figure 4. In contrast to the simple one-proton removal to populate ^{28}Ne, this complex reaction is not selective. Comparison to shell model calculations indicates that this state could correspond to the $1/2^-$, $3/2^-$ or the $5/2^+$ states near the neutron separation energy.

We fit the measured spectrum with an energy-dependent Breit-Wigner lineshape for $l = 1$. An expected width was calculated in the same manner as the ^{28}Ne widths and then fixed at 22 keV for $l = 1$. We also modeled the decay with $l = 2, 3$ lineshapes (fixed widths of 2 keV and 0.2 keV) and similar to ^{28}Ne, the data are insensitive to the orbital angular momentum.

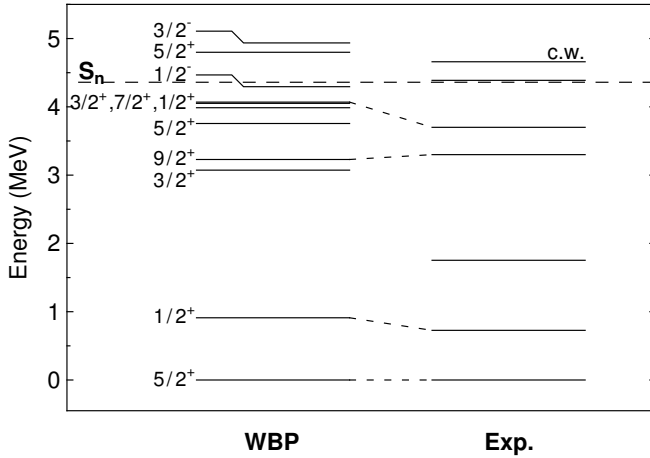Previously, Frank et al.[2] had observed a low-lying

including a population of up to 27% of this resonance are possible within our confidence interval and an example of such a fit is shown in the lower panel of Figure 3. Frank et al. also included unresolvable states at higher energies. Their best fit included a resonance component at an energy of 350 keV excitation energy, similar to the one reported here. Thus we expect that the state measured here corresponds to either the calculated $3/2^-$ state or the $5/2^+$ state.

In summary, we report on evidence for two new unbound states, one at $32(22)$ keV decay energy in the ^{28}Ne $\rightarrow^{27}$Ne $+ n$ system and one at $300(170)$ keV decay energy in the ^{25}F $\rightarrow^{24}$F $+ n$ system. While neither state can be firmly assigned a spin at this time, comparisons to shell model calculations suggest that the state in ^{28}Ne corresponds to a 2^+, 3^+ or 4^+ state whilethe state in ^{25}F could correspond to either a $3/2^-$ or $5/2^+$ state.

FIG. 4. ^{25}F experimental and calculated levels. The measured bound states are from Refs. [30, 31] and the lowest measured unbound state is from Ref. [2] (adjusted relative to the neutron separation energy). The measured state from the current work is denoted with "c.w." The horizontal dashed line indicates the one-neutron separation energy from Ref. [29].

neutron-unbound state at 28(4) keV excitation energy. They argued that the one-proton knockout used to populate ^{25}F in that experiment would selectively populate negative parity states and assigned the low-lying state to the $1/2^-$ state just above the neutron separation energy. In our spectrum, that state is not immediately visible above the non-resonant background. As a test, the resonance was included in the simulation. Its inclusion did not change the position of the 300 keV resonance. Fits

[1] T. Baumann, A. Spyrou, and M. Thoennessen, Rep. Prog. Phys. **75**, 036301 (2012).

[2] N. Frank *et al.*, Phys. Rev. C **84**, 037302 (2011).

[3] G. Christian *et al.*, Phys. Rev. Lett. **108**, 032501 (2012).

[4] G. Christian *et al.*, Phys. Rev. C **85**, 034327 (2012).

[5] S. M. Brown *et al.*, Phys. Rev. C **85**, 011302 (2012).

[6] C. R. Hoffman *et al.*, Phys. Lett. B **672**, 17 (2009).

[7] C. R. Hoffman *et al.*, Phys. Rev. Lett. **100**, 152502 (2008).

[8] M. J. Strongman *et al.*, Phys. Rev. C **80**, 021302 (2009).

[9] C. R. Hoffman *et al.*, Phys. Rev. C **83**, 031303 (2011).

[10] M. D. Bird, S. J. Kenney, J. Toth, H. W. Weijers, J. C. DeKamp, M. Thoennessen, and A. F. Zeller, IEEE Trans. Appl. Super. **15**, 1252 (2005).

[11] B. Luther *et al.*, Nucl. Instrum. Methods A **505**, 33 (2003).

[12] T. Baumann *et al.*, Nucl. Instrum. Methods A **543**, 517 (2005).

[13] A. Schiller *et al.*, Phys. Rev. Lett. **99**, 112501 (2007).

[14] N. Frank, A. Schiller, D. Bazin, W. A. Peters, and M. Thoennessen, Nucl. Instrum. Methods A **580**, 1478 (2007).

[15] A. M. Lane and R. G. Thomas, Rev. Mod. Phys. **30**, 257 (1958).

[16] G. Blanchon, A. Bonaccorso, D. Brink, A. García-Camacho, and N. Vinh-Mau, Nucl. Phys. A **784**, 49 (2007).

[17] B. Jurado *et al.*, Phys. Lett. B **649**, 43 (2007).

[18] B. A. Brown and W. D. M. Rae, MSU-NSCL report (2007).

[19] B. A. Brown and W. A. Richter, Phys. Rev. C **74**, 034315 (2006).

[20] M. Belleguic *et al.*, Phys. Rev. C **72**, 054316 (2005).

[21] J. R. Terry *et al.*, Phys. Lett. B **640**, 86 (2006).

[22] Z. Elekes *et al.*, J. Phys. G: Nucl. Part. Phys. **35**, 014038 (2008).

[23] H. Iwasaki *et al.*, Phys. Lett. B **620**, 118 (2005).

[24] E. Rodriguez-Vieitez, *Structure and Cross Section Data of Neutron-Rich N∼20 Nuclei Produced in Fragmentation and Few-Nucleon Knockout Reactions*, Ph.D. thesis, University of California Berkeley (2007).

[25] Y. Utsuno, T. Otsuka, T. Mizusaki, and M. Honma,

Phys. Rev. C **60**, 054315 (1999).

[26] Y. Utsuno, private communication (2012).

[27] Y. Utsuno, T. Otsuka, T. Glasmacher, T. Mizusaki, and M. Honma, Phys. Rev. C **70**, 044307 (2004).

[28] A. Bohr and B. Mottelson, *Nuclear Structure*, Vol. 1 (W.A. Benjamin, Inc., 1969).

[29] R. B. Firestone, Nuclear Data Sheets **110**, 1691 (2009).

[30] Z. Elekes *et al.*, Phys. Lett. B **599**, 17 (2004).

[31] F. Azaiez, Nucl. Phys. A **704**, 37 (2002).

[32] B. A. Brown, A. Etchegoyen, and W. D. M. Rae, MSU-NSCL report (1988).

[33] E. K. Warburton and B. A. Brown, Phys. Rev. C **46**, 923 (1992).